

PAS10

Why Surface Monitoring of Microseismic Events Works

L. Eisner* (I. of Rock Structure and Mech., Czech Ac. Sc./MSI), A. De La Pena (Microseismic Inc), S. Wessels (Microseismic Inc), W. Barker (Microseismic Inc) & W. Heigl (Apache Corporation)

SUMMARY

Microseismic monitoring can be either carried from the surface or borehole. While noise levels in the borehole are usually much lower than on the surface (typically by a factor of 10), we show that the signal amplitude at the earth's surface is also larger due to a free surface boundary condition (simultaneous observation of both direct and reflected waves) and impedance contrasts at the low-impedance near surface layers. Thus a comparison of detectability of microseismic events between surface and downhole monitoring systems needs to take into consideration amplitude gains in near surface layers. We show a typical example of such gains on a vertical geophone array where the amplitude of the direct P-wave increases by more than a factor of 3 from a 150 m deep geophone to a geophone at the earth's surface. Considering this amplitude gain one can calculate a theoretical detectability between surface and downhole monitoring arrays and we show that surface and downhole monitoring arrays can have approximately similar detectability at distances of a few hundred meters from a monitoring borehole, and that a surface array detects significantly more events at distances beyond 500 meters from a monitoring borehole.

Introduction

Passive seismic monitoring of microseismic events induced by oilfield operations has grown nearly exponentially over the last several years as it provides unique insight into the geomechanical behavior of oil and gas reservoirs. The main objective of such monitoring is to detect and analyze microseismic events (generally with moment release less than $10^{9.1}$ Nm, corresponding to a moment magnitude of zero). This is typically achieved either by deploying seismic sensors into dedicated monitoring wells (e.g., Maxwell et al., 2010), herein called downhole monitoring, or deploying a large number of seismic sensors on the surface or in shallow monitoring boreholes (e.g. Duncan and Eisner, 2010), herein called surface monitoring. For downhole monitoring, typically 8 and 40 geophones are deployed in a single monitoring well (although recently downhole monitoring from multiple monitoring wells is becoming more common), while surface monitoring deploys 900 to 1500 vertical geophones on the earth's surface or 80 to 200 sensors in shallow monitoring holes. While downhole monitoring uses inversion techniques to locate and further analyze microseismic events with signals greater than noise observed on seismic sensors, surface monitoring relies on imaging techniques since the majority of recorded microseismic events have a signal lower than noise on surface geophones.

Recently, Warpinski (2009) pointed out that even by stacking of a large number of seismic sensors the signal-to-noise ratio is 10^7 times lower on surface than on individual downhole sensors 330 m away from a microseismic event at an approximate depth of 3300 m, i.e. at least 3300 m away from the surface sensors. Such calculations seem to be at odds with direct surface observations where signals from microseismic events can be observed simultaneously on downhole and surface geophones (Eisner et al., 2010; Reshetnikov et al., 2010). We show that while surface noise levels are indeed approximately 10 times higher than in dedicated monitor wells (surface noise levels range from 50 to 200 nm/s while downhole noise levels range between 10 to 30 nm/s), the signal on surface or near surface geophones is enhanced by impedance contrasts at shallow layers. This fundamental fact is routinely observed on multiple monitoring sites and probably results from decreased velocity and density in the near surface layers in sedimentary basins.

Case Study

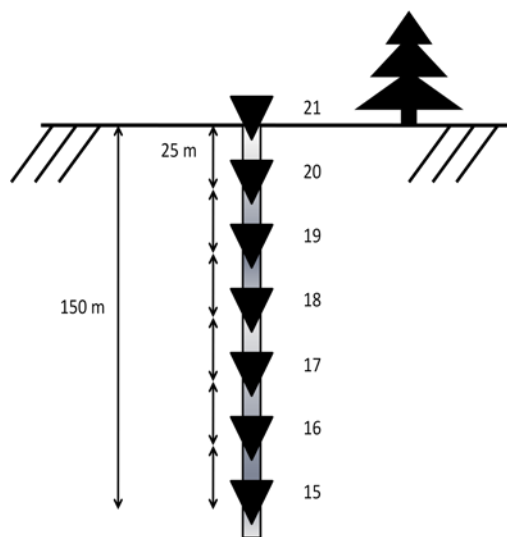


Figure 1, Vertical cross-section of geophones in shallow borehole array. Vertical geophones are represented by inverted triangles. Geophone identification numbers are on the right hand side of the corresponding triangles.

In this study we investigate true amplitudes of seismic signals recorded with geophones in a shallow borehole array during a hydraulic fracture stimulation in the Horn River basin, British Columbia, Canada. The borehole array is part of a larger monitoring array of seven shallow boreholes instrumented with geophones placed at varying depths and on the surface. At least one microseismic event had sufficient signal to produce detectable P-wave arrivals on all vertical geophones without stacking. The move-out of the P-wave arrivals of both surface and shallow borehole geophones is consistent with an event located close to the stimulated interval at a depth exceeding 2000 m. In addition, horizontal components on the shallow borehole geophones show S-wave arrivals consistent with the depth of the stimulated interval and the P-wave amplitude polarity consistent with a strike-slip event. We therefore conclude that the observed seismic signal is caused by induced microseismicity. Figure 1 illustrates the layout of the geophones in a shallow borehole. Figure 2 shows the recorded particle velocity on the 7 geophones in the shallow borehole array shown in Figure 1. Note the P-wave arrives first on geophones 15, 16, and

17 at around 1.4 seconds because the seismic signal originates below the array and propagates up along the array towards the earth's surface. The time delays on the bottom three geophones imply very high apparent velocities – the arrivals are only 4 ms apart which corresponds to a velocity of 6250 m/s. The arrivals on shallower geophones are delayed 12 milliseconds (geophone 17 to 18), 14 milliseconds (geophone 18 to 19 and 19 to 20) and 8 milliseconds (geophone 20 to 21) corresponding to apparent velocities 2000, 1786 and 3125 m/s, respectively. This observation can be explained by a strong P-wave velocity contrast between geophones 17 and 18, i.e. 100 and 75 meters depth, where the velocity decreases by a factor of three. Such a decrease in the near-surface velocities will likely result in strong impedance contrasts thereby increasing amplitudes of the arriving waves at shallower receivers as observed in this study (notice the amplitudes of P-wave on receivers 18, 19, 20 and 21 increase as the wave approaches the free surface). Geophone 21 on the surface has a P-wave amplitude 2.3 times larger than geophone 20. Furthermore, the amplitude on geophone 20 is approximately 1.5 times larger than on geophone 15. The larger amplitude on the surface geophone can be explained by free surface correction (pp. 190 of Aki and Richards, 1980) as the surface geophone records both the direct and reflected waves simultaneously, resulting in an amplitude correction for vertical component of P-wave:

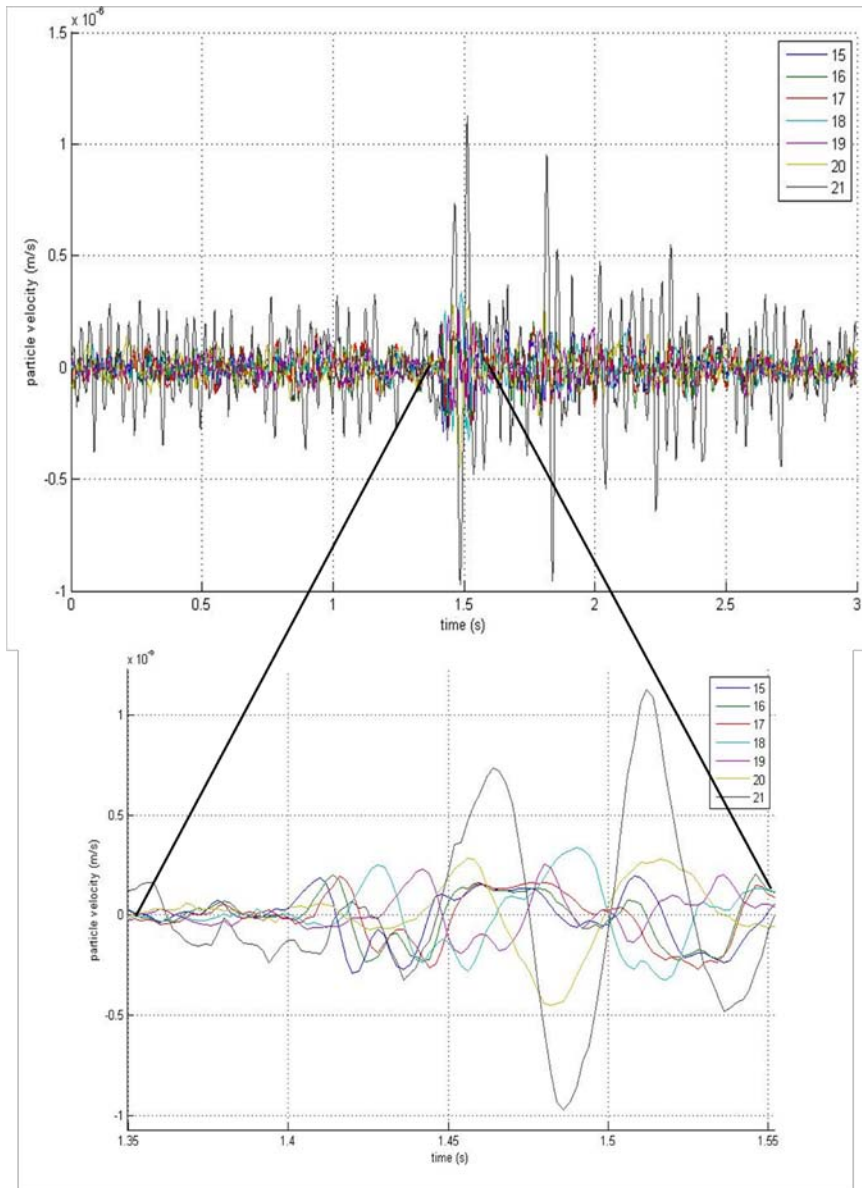


Figure 2 Particle velocity seismograms recorded with the vertical array of geophones illustrated in Figure 1. The lowest receiver is geophone No 15 represented by light blue color, the surface receiver is geophone No 21 represented by black color.

geophone 15. The larger amplitude on the surface geophone can be explained by free surface correction (pp. 190 of Aki and Richards, 1980) as the surface geophone records both the direct and reflected waves simultaneously, resulting in an amplitude correction for vertical component of P-wave:

$$A = \frac{-2 \cos i \left(\frac{1}{\beta^2} - 2p^2 \right)}{\left(\frac{1}{\beta^2} - 2p^2 \right)^2 + \frac{4p^2}{\alpha\beta} \cos i \cos j}, \quad (1)$$

Where α and β represent P- and S-wave particle velocity at the free surface, p is horizontal slowness ($p = \frac{\sin i}{\alpha}$) and i and j are P-wave incident angle and S-wave reflected angle at the free surface. It is easy to see that equation (1) can be reduced to a correction of $A = -2$ for vertical incidence where $p = \sin i = 0$. The additional amplitude increase (i.e. increase of amplitude ratio from 2 to 2.3 between geophones 20 and 21 or increase by a factor of 1.5 between geophones 15 and 20) can be explained by a decrease in impedance between deeper and shallow near-surface layers, which for a normal incidence P-wave can be written in the form of:

$$A = \frac{2z_1}{z_0 + z_1}, \quad (2)$$

where z_0 and z_1 are impedances (velocity times density) of the deep and shallow layers, respectively. The observed increase of signal strength at the near-surface layers contradicts previously assumed signal loss due to near-surface attenuation (e.g. Warpinski 2010, or Shemeta and Anderson, 2010). However, the signal gain at the free surface and near-surface receivers is less than the increase in noise as shown in Figure 2. This is not surprising, as the noise is composed of seismic waves similar to the signal that also reflect at the free surface. In our example, the signal-to-noise ratio on the free surface geophone 21 is approximately 2.5 while the geophone 15 has a signal-to-noise ratio of approximately 3.5. Thus by lowering receivers into a shallow borehole we gained approximately a factor of 1.4 in signal-to-noise ratio (an average over all receivers in this array). The observations made here are not specific to the Horn River basin. Similar observations of signal-to-noise gain at near surface layers have been made in other basins throughout the USA and Europe.

Signal-to-noise ratio between downhole and surface monitoring

This observation may now be used to determine relative detectability of microseismic events from downhole and surface monitoring arrays. To do so, we compare signal-to-noise ratios of surface and downhole arrays. The resulting signal-to-noise ratio of hypothetical microseismic events detected with downhole and surface monitoring is dependent on many additional factors that we shall try to account for in this section. We assume that we have a surface array of 1000 geophones deployed to monitor microseismic events at a depth of 2000 m. We compare the average signal-to-noise ratio of the stacked amplitude from the surface array to the signal-to-noise ratio on a virtual downhole geophone at 200 m distance from the microseismic event (no stacking is applied as we assume P- and S-waves need to be picked individually on each geophone). The geometrical spreading between downhole and individual surface geophones will decrease the signal by a factor of approximately 10 as amplitude decays at a rate of 1/distance in a homogeneous medium. This factor is an upper bound as the lower velocities near the surface usually cause the signal to focus towards the surface. Attenuation will further decrease the signal on both downhole and surface geophones, however, surface monitoring uses lower frequency signals (around 20-40 Hz, see Duncan and Eisner, 2010 for more details) and will experience less attenuation per unit distance than a higher frequency signal observed on downhole geophones (typically >100 Hz). Then, assuming an effective attenuation factor of $Q=100$ and peak frequencies of 30 Hz and 100 Hz for surface and downhole, respectively, results in a surface to downhole signal amplitude ratio of 0.7.

The source mechanism also affects both downhole and surface signals. We have computed an average P-wave amplitude from strike-slip and dip-slip earthquakes at multiple azimuths for a vertical downhole array and surface FracStar[®] array resulting in a very similar average amplitudes on both arrays. Thus we can neglect the effect of source mechanisms on the differing signal-to-noise ratio between surface and downhole monitoring. Also, we neglect transmission losses (these seem to be less significant than transmission gains as shown above) and attenuation caused by near-surface layers. We assume that the free surface increases signal by approximately a factor of 3 as observed on the shallow borehole array of Figure 1 (recall the free surface (near vertical) correction and impedance contrast). Finally, we assume that the stacked signal on the surface is increased by a factor equal to

the square root of the number of receivers ($\sqrt{1000}$) and calculate the average signal-to-noise ratio

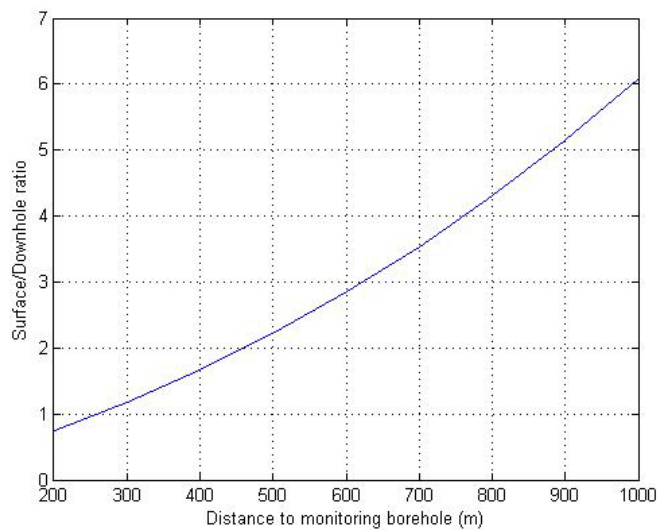


Figure 3 Predicted ratio of average stacked surface to downhole arrays signal-to-noise ratios of microseismic events.

microseismic events with a relatively small number of surface geophones. The computed ratio of the number of detected events by downhole and surface arrays for a given geometry shows that a surface array detects approximately the same number of microseismic events as a downhole array located at a distance of 200 m from the treatment interval and more events if the treatment interval is greater than 500 m from the downhole array.

Acknowledgements

We would like to thank EnCana and Apache Corporation for the release of this dataset.

References:

- Aki, K., Richards, P.G., 1980. Quantitative Seismology, Freeman and Co., New York
- Duncan, P. and L. Eisner, (2010): Reservoir characterization using surface microseismic monitoring. *Geophysics*, 75, No. 5, pp. 75A139–75A146; doi:10.1190/1.3467760.
- Maxwell S., J. Rutledge, R. Jones, M. Fehler, (2010): Petroleum Reservoir Characterization Using Downhole Microseismic Monitoring. *Geophysics*, 75, No. 5, 75A129-75A137; doi: 10.1190/1.3477966.
- Warpinski N., (2010): The physics of surface microseismic monitoring. Pinnacle Fracture Diagnostics Tech Update, H07119 05/10. http://www.pinntech.com/pubs/TU/TU10_MS.pdf, accessed October 26, 2010.
- Eisner, L, B. J. Hulsey, P. Duncan, D. Jurick, H. Werner, W. Keller. 2010: Comparison of surface and borehole locations of induced microseismicity. *Geophysical Prospecting*, doi: 10.1111/j.1365-2478.2010.00867.x
- Reshetnikov A., Kummerow J., Buske S., and Shapiro, S.A., 2010: Microseismic imaging from a single geophone: KTB. *SEG Expanded Abstracts* 29, 2070, DOI:10.1190/1.3513252
- Shemeta J. and P. Anderson, 2010: It's a matter of size: Magnitude and moment estimates for microseismic data. *The Leading Edge*, 29, pp. 296 – 302. Doi 10.1190/1.3353726